Acta Mechanica 164, 1–13 (2003)
DOI 10.1007/s00707-003-0015-8

Acta Mechanica
Printed in Austria

Large deflection analysis of beams with variable stiffness

J. T. Katsikadelis and **G. C. Tsiatas,** Athens Greece

Received July 29, 2002; revised March 31, 2003
Published online: August 7, 2003

Summary. In this paper, the Analog Equation Method (AEM), a BEM-based method, is employed to the nonlinear analysis of a *Bernoulli-Euler* beam with variable stiffness undergoing large deflections, under general boundary conditions which maybe nonlinear. As the cross-sectional properties of the beam vary along its axis, the coefficients of the differential equations governing the equilibrium of the beam are variable. The formulation is in terms of the displacements. The governing equations are derived in both deformed and undeformed configuration and the deviations of the two approaches are studied. Using the concept of the analog equation, the two coupled nonlinear differential equations with variable coefficients are replaced by two uncoupled linear ones pertaining to the axial and transverse deformation of a substitute beam with unit axial and bending stiffness, respectively, under fictitious load distributions. Besides the effectiveness and accuracy of the developed method, a significant advantage is that the displacements as well as the stress resultants are computed at any cross-section of the beam using the respective integral representations as mathematical formulae. Several beams are analyzed under various boundary conditions and loadings to illustrate the merits of the method as well as its applicability, efficiency and accuracy.

1 Introduction

In recent years a need has been raised in engineering practice to predict accurately the nonlinear response of beams, especially when the properties of their cross section are variable. The nonlinearity results from retaining the square of the slope in the strain-displacement relations. In this case the transverse deflection influence the axial force and the resulting equations, governing the response of the beam, are coupled nonlinear with variable coefficients. Moreover, the pertinent boundary conditions of the problem are in general nonlinear. Closed form solutions cannot be obtained when general boundary conditions are considered unless these are simplified on the basis of certain mathematical adjustments. Therefore recourse to numerical solutions is inevitable. Among, them the FEM has been widely used for nonlinear analysis of beams with constant cross-section having both geometric and material nonlinearities [1], [2]. Nevertheless, in FEM, beams with nonuniform cross-section must be approximated by a large number of small uniform elements replacing the continuous variation with a step law. In this way it is always possible to obtain acceptable results and the error can be reduced as much as desired by refining the mesh, at the expense of computational cost. On the other hand the application of the BEM to the analysis of beams is restricted only to linear problems. Its first application date back to the work of Banerjee and Butterfield [3], who developed the BEM for the one-dimensional problem and applied it to the analysis of the Bernoulli-Euler beam under static loads. Providakis and Beskos [4] applied the BEM to the dynamic problem of Bernoulli-Euler beams. Recently, the BEM was employed for the linear static analysis of Timoshenko's beams [5].

In this paper, an accurate direct solution to the governing coupled nonlinear differential equations is developed, which permits the treatment also of nonlinear boundary conditions. The governing equations are derived in both the deformed and the undeformed configuration. The solution method is based on the concept of the analog equation [6] as it was developed for the solution of nonlinear problems [7]. According to this concept, the two coupled nonlinear differential equations are replaced by two equivalent uncoupled linear ones pertaining to the axial and transverse deformation of a substitute beam with unit axial and bending stiffness subjected to fictitious load distributions under the same boundary conditions. Subsequently, the fictitious loads are established using the BEM for linear one-dimensional differential equations and, thus, the displacements and their derivatives are established from the respective integral representation. Several beams are analyzed under various boundary conditions and load distributions, which illustrate the method and demonstrate its efficiency and accuracy. Moreover, useful conclusions are drawn from the comparison of the two sets of equations derived on basis of the deformed and undeformed configuration. The latter one is usually adopted in the literature to reduce the nonlinearity of the problem.

2 Governing equations

Consider an initially straight beam of length l having variable axial stiffness EA and bending stiffness EI , which may result from variable cross-section, $A = A(x)$, and/or from inhomogeneous linearly elastic material, $E = E(x)$; $I = I(x)$ is the moment of inertia of the cross-section. The x-axis coincides with the neutral axis of the beam, which is bent in its plane of symmetry xz under the combined action of the distributed loads $p_x = p_x(x)$ and $p_z = p_z(x)$ in the x- and z-direction, respectively. The large deflection theory result from the nonlinear kinematic relation, which retains the square of the slope of the deflection, while the strain component remains still small compared with the unity. Thus, taking into account that $u_{,x}^2 \ll u_{,x}$ we have

$$\varepsilon_x(x,z) = u_{,x} + \tfrac{1}{2} w_{,x}^2 + z\kappa, \tag{1}$$

where $u = u(x)$ and $w = w(x)$ are displacements along the x- and z-axis, respectively, and κ is the curvature of the deflected axis.

Referring to the equilibrium of the deformed element (see Fig. 1) the following relations are derived:

$$p_x^* = p_x dx/ds, \quad p_z^* = p_z dx/ds, \quad m^* = m dx/ds, \tag{2}$$

$$ds = \sqrt{(1 + u_{,x})^2 + w_{,x}^2}\, dx, \tag{3}$$

$$\cos\theta = \frac{1 + u_{,x}}{\sqrt{(1 + u_{,x})^2 + w_{,x}^2}}, \quad \sin\theta = \frac{w_{,x}}{\sqrt{(1 + u_{,x})^2 + w_{,x}^2}} \tag{4}$$

which for the case of moderate large deflections ($u_{,x}, w_{,x}^2 \ll 1$) become

$$p_x^* = p_x, \quad p_z^* = p_z, \quad m^* = m, \tag{5}$$

$$ds = dx, \tag{6}$$

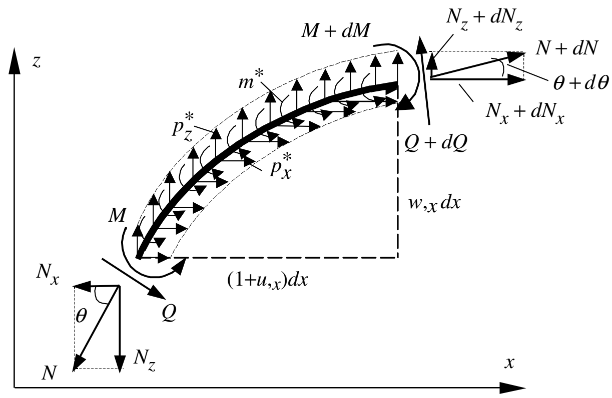

Fig. 1. Forces and moments acting on the deformed element

$$\cos\theta \simeq 1, \quad \sin\theta \simeq w_{,x} \simeq \theta. \tag{7}$$

Moreover, the strain $\varepsilon_0 = \varepsilon_x(x, 0)$ at the x-axis and the curvature $\kappa = \kappa(x)$ are given as

$$\varepsilon_0 = u_{,x} + \frac{1}{2} w_{,x}^2, \tag{8}$$

$$\kappa = \frac{d\theta}{ds} \simeq \theta_{,x} \simeq w_{,xx}\,. \tag{9}$$

Therefore, the stress resultants, that is the axial force and the bending moment are given as

$$N = EA\left(u_{,x} + \frac{1}{2} w_{,x}^2\right), \tag{10}$$

$$M = -EI w_{,xx}\,. \tag{11}$$

From Fig. 1, we have

$$N_x = N\cos\theta - Q\sin\theta \simeq N - Q w_{,x}\,, \tag{12}$$

$$N_z = N\sin\theta + Q\cos\theta \simeq N w_{,x} + Q. \tag{13}$$

The governing equations are derived by considering the equilibrium of the deformed element. Thus, referring to Fig. 1 we obtain:

$$N_{x,x} = -p_x, \tag{14}$$

$$N_{z,x} = -p_z, \tag{15}$$

$$M_{,x} = Q + m. \tag{16}$$

Substituting Eqs. (12) and (13) into Eqs. (14) and (15) and using Eq. (16) to eliminate Q, we obtain:

$$N_{,x} - (M_{,x}\, w_{,x})_{,x} + (m w_{,x})_{,x} = -p_x, \tag{17}$$

$$M_{,xx} + (N w_{,x})_{,x} = -p_z + m_{,x} \tag{18}$$

which by virtue of Eqs. (10) and (11) become

$$\left[EA\left(u_{,x} + \tfrac{1}{2} w_{,x}^2\right)\right]_{,x} + (EI w_{,xxx}\, w_{,x})_{,x} + (m w_{,x})_{,x} = -p_x, \tag{19}$$

$$(EI w_{,xx})_{,xx} - \left[EA\left(u_{,x} + \tfrac{1}{2} w_{,x}^2\right) w_{,x}\right]_{,x} = p_z + m_{,x}\,. \tag{20}$$

The pertinent boundary conditions are:

$$a_1 u(0) + a_2 N_x(0) = a_3, \tag{21}$$

$$\bar{a}_1 u(l) + \bar{a}_2 N_x(l) = \bar{a}_3, \tag{22}$$

$$\beta_1 w(0) + \beta_2 N_z(0) = \beta_3, \tag{23}$$

$$\bar{\beta}_1 w(l) + \bar{\beta}_2 N_z(l) = \bar{\beta}_3, \tag{24}$$

$$\gamma_1 w_{,x}(0) + \gamma_2 M(0) = \gamma_3, \tag{25}$$

$$\bar{\gamma}_1 w_{,x}(l) + \bar{\gamma}_2 M(l) = \bar{\gamma}_3, \tag{26}$$

where $a_k, \bar{a}_k,\ \beta_k, \bar{\beta}_k,\ \gamma_k,\ \bar{\gamma}_k (k = 1, 2, 3)$ are given constants. Equations (21)–(26) describe the most general boundary conditions associated with the problem and can include elastic support or restrain. They are linear except in the case of non vanishing end forces N_x, N_z, e.g., if at $x = 0$ it is $a_2 \neq 0$, $|a_1| + |a_3| \neq 0$ and/or $\beta_2 \neq 0$, $|\beta_1| + |\beta_3| \neq 0$.

The term $Qw_{,x} = EIw_{,xxx} w_{,x}$, which appears in Eq. (19), expresses the influence of the shear force Q on N_x. The presence of this term increases highly the difficulty of the solution. The existing solutions circumvent this difficulty by neglecting this nonlinear term. This assumption yields $N_x \simeq N$ and it is true if the equilibrium is considered in the undeformed configuration. Thus the governing equations are simplified as

$$\left[EA\left(u_{,x} + \tfrac{1}{2} w_{,x}^2\right)\right]_{,x} + (m w_{,x})_{,x} = -p_x, \tag{27}$$

$$(EIw_{,xx})_{,xx} - \left[EA\left(u_{,x} + \tfrac{1}{2} w_{,x}^2\right) w_{,x}\right]_{,x} = p_z + m_{,x}\,, \tag{28}$$

while the boundary conditions become:

$$a_1 u(0) + a_2 N(0) = a_3, \tag{29}$$

$$\bar{a}_1 u(l) + \bar{a}_2 N(l) = \bar{a}_3, \tag{30}$$

$$\beta_1 w(0) + \beta_2 N_z(0) = \beta_3, \tag{31}$$

$$\bar{\beta}_1 w(l) + \bar{\beta}_2 N_z(l) = \bar{\beta}_3, \tag{32}$$

$$\gamma_1 w_{,x}(0) + \gamma_2 M(0) = \gamma_3, \tag{33}$$

$$\bar{\gamma}_1 w_{,x}(l) + \bar{\gamma}_2 M(l) = \bar{\gamma}_3. \tag{34}$$

In this paper, this simplifying assumption is investigated by solving both sets of governing equations and useful conclusions are drawn regarding its validity.

3 The AEM solution

Equations (19) and (20) are solved using the AEM, which for the problem at hand is applied as follows. Let $u = u(x)$ and $w = w(x)$ be the sought solutions, which are two and four times differentiable, respectively, in $(0, l)$. Noting that Eqs. (19) and (20) are of the second order with respect to u and of fourth order with respect to w, we obtain by differentiating the following analog equations:

$$u_{,xx} = b_1(x), \tag{35}$$

$$w_{,xxxx} = b_2(x), \tag{36}$$

where b_1, b_2 are fictitious loads. Equations (35) and (36) indicate that the solution of Eqs. (19) and (20) can be established by solving Eqs. (35) and (36) under the boundary conditions (21)–(26), provided that the fictitious load distributions b_1, b_2 are first determined.

The fictitious loads are determined by developing a procedure based on the boundary integral equation method for one-dimensional problems. Thus, the integral representations of the solutions of Eqs. (35) and (36) are written as

$$u(x) = c_1 x + c_2 + \int_a^l G_1(x,\xi) b_1(\xi) d\xi, \tag{37}$$

$$w(x) = c_3 x^3 + c_4 x^2 + c_5 x + c_6 + \int_a^l G_2(x,\xi) b_2(\xi) d\xi, \tag{38}$$

where $c_i (i = 1, 2, \ldots 6)$ are arbitrary integration constants to be determined from the boundary conditions and $G_i(x,\xi)(i = 1, 2)$ are the fundamental solutions of Eqs. (35) and (36), that is particular singular solutions of the following equations:

$$G_{1,xx} = \delta(x - \xi), \tag{39}$$

$$G_{2,xxxx} = \delta(x - \xi) \tag{40}$$

with $\delta(x - \xi)$ being the Dirac function.

Integration of Eqs. (39) and (40) yields [3]

$$G_1 = \tfrac{1}{2}|x - \xi|, \tag{41}$$

$$G_2 = \tfrac{1}{12}|x - \xi|(x - \xi)^2. \tag{42}$$

The derivatives of u and w are obtained by direct differentiation of Eqs. (37) and (38). Thus, we have

$$u_{,x}(x) = c_1 + \int_0^l G_{1,x}(x,\xi) b_1(\xi) d\xi, \tag{43}$$

$$u_{,xx}(x) = b_1(x), \tag{44}$$

$$w_{,x}(x) = 3c_3 x^2 + 2c_4 x + c_5 + \int_0^l G_{2,x}(x,\xi) b_2(\xi) d\xi, \tag{45}$$

$$w_{,xx}(x) = 6c_3 x + 2c_4 + \int_0^l G_{2,xx}(x,\xi) b_2(\xi) d\xi, \tag{46}$$

$$w_{,xxx}(x) = 6c_3 + \int_0^l G_{2,xxx}(x,\xi) b_2(\xi) d\xi, \tag{47}$$

$$w_{,xxxx}(x) = b_2(x). \tag{48}$$

Substituting the derivatives in Eqs. (19) and (20) yields the equations, from which the fictitious sources b_1 and b_2 can be determined. This process can be implemented only numerically as follows.

The interval $(0, l)$ is divided into N equal elements, having length l/N. Thus, the integral equations (37) and (38) are written as

$$u(x) = c_1 x + c_2 + \sum_{j=1}^{N} \int_j G_1(x, \xi) b_1(\xi) d\xi, \tag{49}$$

$$w(x) = c_3 x^3 + c_4 x^2 + c_5 x + c_6 + \sum_{j=1}^{N} \int_j G_2(x, \xi) b_2(\xi) d\xi, \tag{50}$$

where the symbol $\int_j$ indicates the integral on the j-element. Subsequently, the fictitious sources are approximated on each integration interval using constant, linear or quadratic variation. In this investigation, the constant element is employed. That is, the fictitious source is assumed constant on the element and its nodal value is placed at the midpoint of the element. The integration of the kernels is performed analytically.

Using this discretization and applying Eqs. (43)–(50) to the N nodal points, we obtain:

$$\mathbf{u} = c_1 \mathbf{x}_1 + c_2 \mathbf{x}_0 + \mathbf{G_1} \mathbf{b}_1, \tag{51}$$

$$\mathbf{u}_{,\mathbf{x}} = c_1 \mathbf{x}_0 + \mathbf{G_1}_{,\mathbf{x}} \mathbf{b}_1, \tag{52}$$

$$\mathbf{u}_{,\mathbf{xx}} = \mathbf{b}_1, \tag{53}$$

$$\mathbf{w} = c_3 \mathbf{x}_3 + c_4 \mathbf{x}_2 + c_5 \mathbf{x}_1 + c_6 \mathbf{x}_0 + \mathbf{G_2} \mathbf{b}_2, \tag{54}$$

$$\mathbf{w}_{,\mathbf{x}} = 3c_3 \mathbf{x}_2 + 2c_4 \mathbf{x}_1 + c_5 \mathbf{x}_0 + \mathbf{G_2}_{,\mathbf{x}} \mathbf{b}_2, \tag{55}$$

$$\mathbf{w}_{,\mathbf{xx}} = 6c_3 \mathbf{x}_1 + 2c_4 \mathbf{x}_0 + \mathbf{G_2}_{,\mathbf{xx}} \mathbf{b}_2, \tag{56}$$

$$\mathbf{w}_{,\mathbf{xxx}} = 6c_3 \mathbf{x}_0 + \mathbf{G_2}_{,\mathbf{xxx}} \mathbf{b}_2, \tag{57}$$

$$\mathbf{w}_{,\mathbf{xxxx}} = \mathbf{b}_2, \tag{58}$$

where $\mathbf{G_1}$, $\mathbf{G_1}_{,\mathbf{x}}, \ldots \mathbf{G_2}_{,\mathbf{xxx}}$ are $N \times N$ known matrices, originating from the integration of the kernels $G_1(x, \xi)$, $G_2(x, \xi)$ and their derivatives on the elements; $\mathbf{u}$, $\mathbf{u}_{,\mathbf{x}}, \ldots$ $\mathbf{w}_{,\mathbf{xxxx}}$ are $N \times 1$ vectors including the values of u , w and their derivatives at the nodal points; $\mathbf{b_1}$, $\mathbf{b_2}$ are also $N \times 1$ vectors containing the values of the fictitious loads at the nodal points and $\mathbf{x}_k = \left\{x_1^k, x_2^k, \ldots x_N^k\right\}^T$ are vectors containing the k-th power of the abscissas of the nodal points.

Finally, collocating Eqs. (19) and (20) at the N nodal points and substituting the derivatives from Eqs. (51)–(58) yields the following equations:

$$\mathbf{F}_1(\mathbf{b}_1, \mathbf{b}_2, \mathbf{c}) = \mathbf{p}_x, \tag{59}$$

$$\mathbf{F}_2(\mathbf{b}_1, \mathbf{b}_2, \mathbf{c}) = \mathbf{p}_z, \tag{60}$$

where $\mathbf{F}_i(\mathbf{b}_1, \mathbf{b}_2, \mathbf{c})$ are generalized stiffness vectors and $\mathbf{c} = \{c_1, c_2, \ldots c_6\}^T$. Equations (59) and (60) constitute a system of $2N$ nonlinear algebraic equations with $2N + 6$ unknowns. The required six additional equations result from the boundary conditions. Thus, after substituting the relevant derivatives into Eqs. (21)–(26), we obtain:

$$\mathbf{f}_i(\mathbf{b}_1, \mathbf{b}_2, \mathbf{c}) = \mathbf{0} \quad (i = 1, 2, \ldots 6). \tag{61}$$

The nonlinear equations (59)–(61) have been solved numerically to yield $\mathbf{b}_1, \mathbf{b}_2$ and $\mathbf{c}$ by minimizing the function

$$S(\mathbf{b_1}, \mathbf{b_2}, \mathbf{c}) = \sum_{i=1}^{N} \left\{ \left[F_1^i(\mathbf{b_1}, \mathbf{b_2}, \mathbf{c}) - p_x^i\right]^2 + \left[F_2^i(\mathbf{b_1}, \mathbf{b_2}, \mathbf{c}) - p_z^i\right]^2 \right\} + \sum_{j=1}^{6} f_i(\mathbf{b_1}, \mathbf{b_2}, \mathbf{c})^2. \tag{62}$$

3.1 Treatment of discontinuities

(a) If the loading is discontinuous at a nodal point, the mean value can be employed to restore the continuity. The results are highly improved by adjusting the smoothing curve, e.g.,

$$p(x) = \frac{p_1 + p_2}{2} + \frac{p_2 - p_1}{2} \sin \frac{\pi(x - x_0)}{2\varepsilon}, \quad x_0 - \varepsilon \le x \le \varepsilon + x_0. \tag{63}$$

(b) The concentrated force P at a point $x = x_0$ can be represented by a bell shaped continuous function extended on a small region of length 2ε, e.g.,

$$p(x) = \frac{P}{2\varepsilon} \left[1 + \cos \frac{\pi(x - x_0)}{2\varepsilon} \right], \quad x_0 - \varepsilon \le x \le \varepsilon + x_0, \tag{64}$$

where

$$\int_{x_0-\varepsilon}^{x_0+\varepsilon} p(x)dx = P. \tag{65}$$

4 Numerical examples

On the base of the procedure described in previous section a FORTRAN program has been written for the nonlinear analysis of beams with arbitrarily varying stiffness. In all examples the results have been obtained using $N = 21$ elements, which are enough to ensure the convergence of the solution procedure (see Table 1). Finer elements have been used in the neighborhood of the concentrated load.

4.1 Uniform cross-section. Concentrated load

For the comparison with existing results, a fixed-fixed beam with uniform rectangular cross section $b \times h$ and length $l = 0.508$ m has been analyzed under a concentrated force acting at

Table 1. Numerical results at the centre of the beam, in example 4.3, for various values of N. Thickness variation case (b)

	Hinged-hinged			Fixed-hinged		
	$N = 21$	$N = 31$	$N = 41$	$N = 21$	$N = 31$	$N = 41$
u (m)	−0.00245	−0.00241	−0.00239	0.00218	0.00218	0.00219
w (m)	0.56088	0.56022	0.55998	0.47019	0.46874	0.46824
N_x (kN)	40409	40414	40416	26405	26401	26398
N_z (kN)	19.967	31.327	35.454	1903.5	1916.0	1920.5
M (kNm)	14544	14535	14531	15449	15418	15408

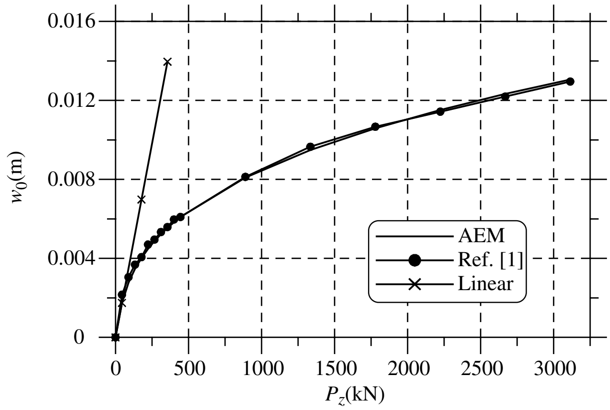

Fig. 2. Central deflection versus load in example 4.1

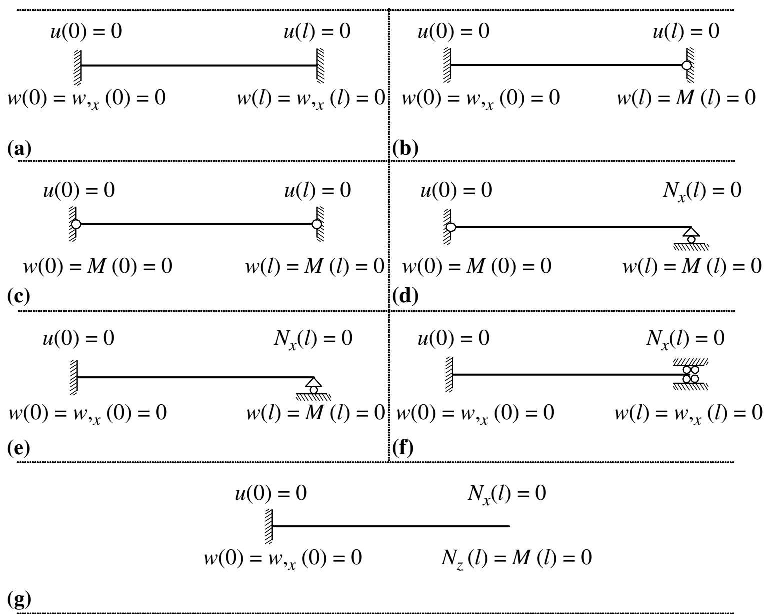

Fig. 3. Boundary conditions in example 4.2

the midspan of the beam. The employed data are: $E = 2.07 \times 10^8$ kN/m^2, $b = 0.0254$ m and $h = 0.003175$ m. Mondkar and Powell [1] have also studied this problem using five eight-node plane stress elements to model one-half of the beam, with 2×2 Gauss quadrature integration. The central deflection w_0 versus the concentrated load P_z is shown in Fig. 2, as compared with the existing solution. The results are in excellent agreement.

4.2 Uniform cross-section. Distributed load

A steel **I**-section beam with length $l = 10.0$ m has been studied using both sets of equations referred to deformed and undeformed configuration. The cross-section is constructed from a pair of identical flange plates $b = 300$ mm wide by $t_f = 30$ mm thick and a web plate $t_w = 12$ mm thick with height $h_w = 500$ mm. The employed data are: $E = 2.1 \times 10^8$ kN/m^2, $p_x = 0$, $m = 0$. The examined boundary conditions are depicted in Fig. 3. The distributed load

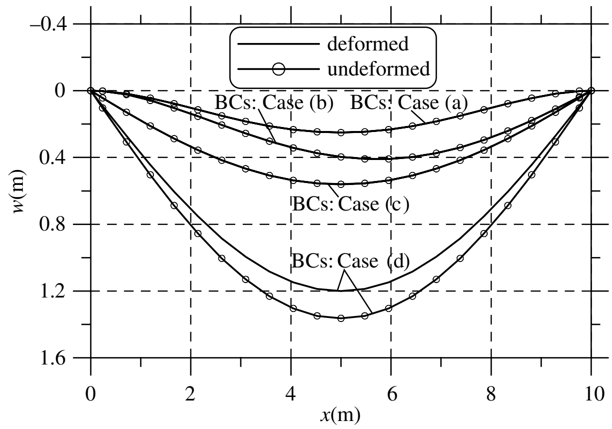

Fig. 4. Profile of the displacement w in example 4.2

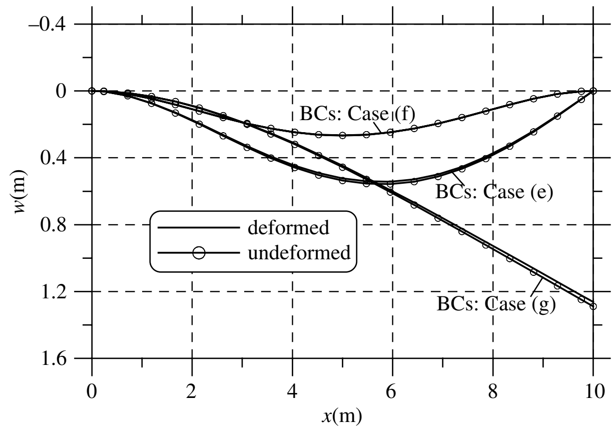

Fig. 5. Profile of the displacement w in example 4.2

$p_z = 3000$ kN/m was used except from the last case where it was taken $p_{z0} = 300$ kN/m. The profiles of the displacement w are shown in Figs. 4 and 5. From these figures, we conclude that for axially immovable ends the deviation between the two sets of governing equations is negligible. However, for axially movable ends the deviation may be appreciable. The same conclusion can be drawn from the profile of the ratio $Qw_{,x}/N$. That is, the ratio $Qw_{,x}/N$ for fixed-fixed ends is small (see Fig. 6), while for pinned-roller ends this ratio approaches the value of 1 as it was anticipated. Figure 7 shows the profiles of the stress resultants in the case of pinned-roller ends, from which we conclude that the axial force N may be appreciable, while it is ignored in the simplified theory, $N \simeq N_x = 0$.

4.3 Variable cross-section. Distributed loads

The steel **I**-section beam of example 4.2 has been studied under varying web height $h_w(x)$. Two cases are considered: (a) constant web height, $h_w = h_w(0)$, and (b) linearly varying web height, $h_w = h_w(0)(0.5 + x/l)$. In both cases the volume of the material, i.e., $V = [t_w h_w(0) + 2t_f b]l$, was kept constant. The employed data are: $p_z = 3000$ kN/m, $p_x = 100$ kN/m and $m = 0$. Two types of boundary conditions are considered: (i) hinged-hinged, and (ii) fixed-hinged. The results for both cases of material distribution are presented in Figs. 8–10. Moreover, numerical results at the centre of the beam are presented in Table 1, for various values of N, from which the convergence and stability of the AEM is concluded. It is apparent that 21 elements give good results.

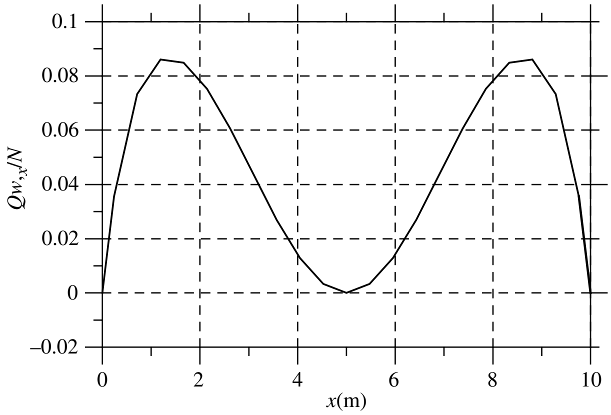

Fig. 6. Profile of the ratio $Qw_{,x}/N$ in example 4.2. Boundary conditions: Case (a)

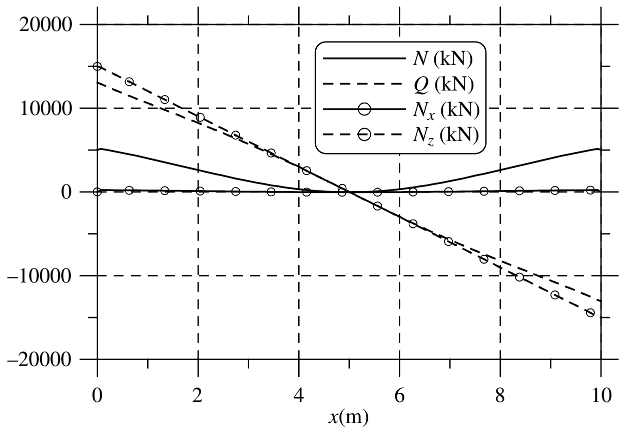

Fig. 7. Profile of the stress resultants in example 4.2. Boundary conditions: Case (d)

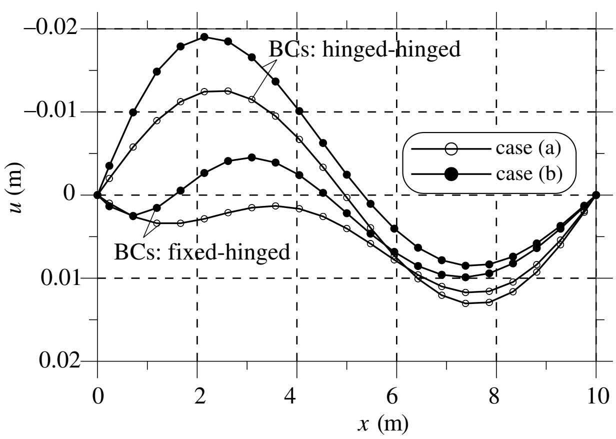

Fig. 8. Profile of the displacement u in example 4.3

4.4 Variable cross-section. Distributed loads and moments

A fixed-fixed beam with length $l = 1.0$ m, has been analyzed. The employed data are: $E = 2.1 \times 10^8$ kN/m^2 , $b = 0.01$ m, $h_0 = 0.03$ m. Two cases of thickness variation and load distributions have been studied (a) $h = h_0$ with $p_x = 0,\ p_z = 2500$ kN/m, $m = 0$ and (b) $h = h_0(1/2 + x/l)$ with $p_x = 1000$ kN/m, $p_z = 2500$ kN/m and the linearly varying distributed

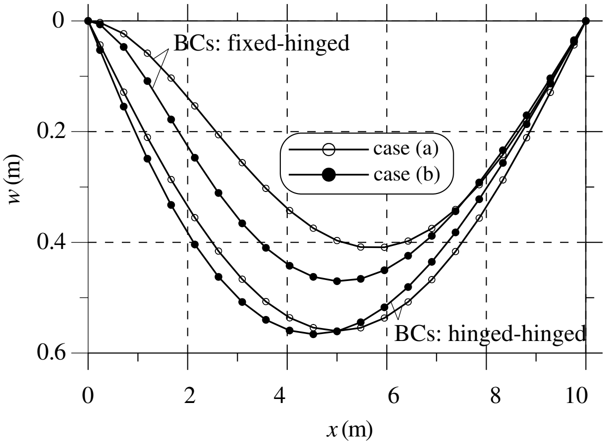

Fig. 9. Profile of the displacement w in example 4.3

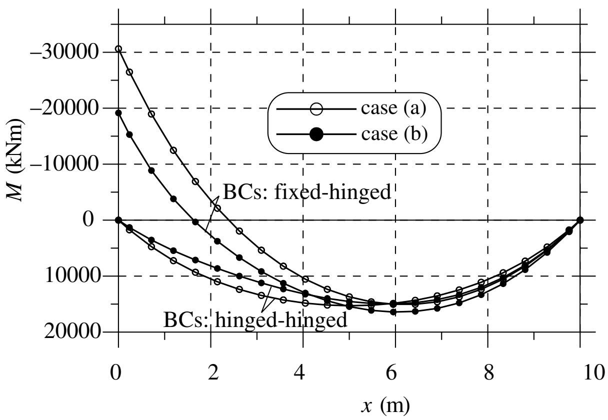

Fig. 10. Profile of the bending moment M in example 4.3

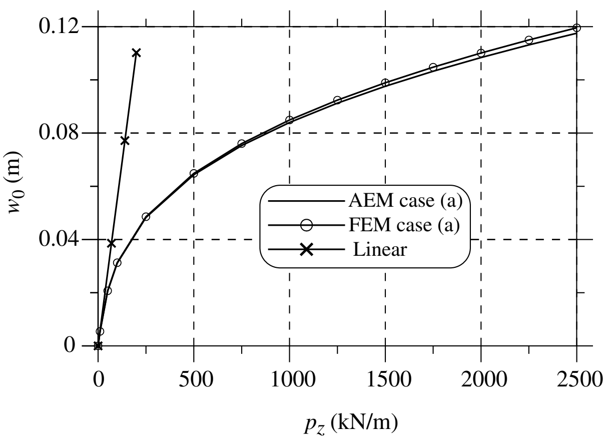

Fig. 11. Central deflection versus load in example 4.4

moment $m = 100x$ (kNm)/m. In both cases of material distribution the volume V of the material has been kept unchanged, that is $V = bh_0 l$. The results are shown in Figs. 11 and 12 for both cases. Comparison of the results with a FEM solution was possible only in case (a) using the NASTRAN code.

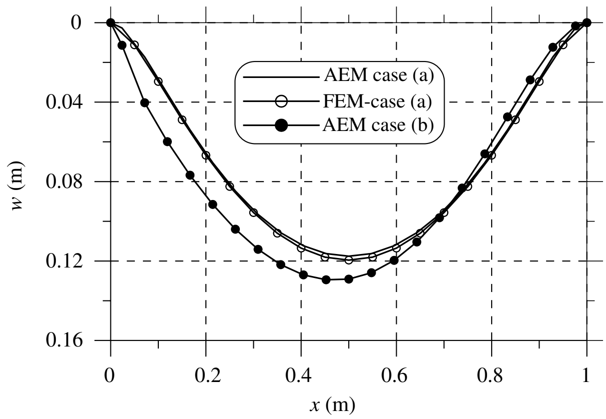

Fig. 12. Profile of the displacement w in example 4.4

5 Conclusions

In this paper, a direct solution to static problem of beams with variable stiffness undergoing large deflections has been presented. The governing equations have been derived considering the equilibrium in the deformed configuration. The presented solution is based on the concept of the analog equation, which converts the two coupled nonlinear equations with variable coefficients into two uncoupled linear ones with fictitious loads. These equations are subsequently solved using the one-dimensional integral equation method. From the presented analysis and the numerical examples the following main conclusions can be drawn: (a) simple fundamental solutions are employed to derive the integral representation of the solution; (b) the displacements and the stress resultants are computed at any point using the respective integral representation as a mathematical formula; (c) the numerical solution exhibits stability and a small number of constant elements are adequate to obtain accurate results for the displacements and the stress resultants; (d) the influence of the shear force on the axial force may be appreciable in the case of axially movable ends. Therefore inaccuracies may result, if the response of the system is obtained using the simplified equations resulting from the equilibrium of the undeformed element.

References

[1] Mondkar, D. P., Powell, G. H.: Finite element analysis of nonlinear static and dynamic response. Int. J. Num. Meth. Enginng. **11,** 499–520 (1977).

[2] Yang, T. Y., Saigal, S.: A simple element for static and dynamic response of beams with material and geometric nonlinearities. Int. J. Num. Meth. Enginng **20,** 851–867 (1984).

[3] Banerjee, P. K., Butterfield R.: Boundary element methods in engineering science. London: McGraw-Hill 1981.

[4] Providakis, C. P., Beskos, D. E.: Dynamic analysis of beams by the boundary element methods. Comp. Struct. **22,** 957–964 (1986).

[5] Antes, H.: Fundamental solution and integral equations for Timoshenko beams. Comp. Struct. **81,** 383–396 (2003).

[6] Katsikadelis, J. T.: The analog equation method-A powerful BEM-based solution technique for solving linear and nonlinear engineering problems. In: Boundary elements XVI, pp. 167–182. Southampton: CLM Publications 1994.

[7] Katsikadelis, J. T., Nerantzaki, M. S.: The boundary element method for nonlinear problems. Engng. Anal. Bound. Elements **23,** 365–373 (1999).

Authors' address: J. T. Katsikadelis and G. C. Tsiatas, School of Civil Engineering, National Technical University of Athens, GR-15773, Greece (E-mail: jkats@central.ntua.gr)